

D-dimer level. The patient's serum ferritin level of  $>40\,000\ \mu\text{g/L}$  was extremely elevated (normal range, 3–166  $\mu\text{g/L}$ ). Urinary analysis showed proteinuria and microhematuria. The blood culture was sterile. Computed tomography of the chest and abdomen showed right axillary lymphadenopathy and bilateral renal swelling; however, there was no evidence of hepatosplenomegaly. Bone marrow aspiration revealed mildly hypocellular marrow with an increase in levels of activated histiocytes and hemophagocytes. The patient's condition deteriorated rapidly on the day following admission with the appearance of macrohematuria and a massive amount of tarry stool. Death occurred on the third day of hospitalization.

Serum was used for virus isolation using Vero and *Felis catus* whole fetus (Fcwf-4) cells. Cytopathic effect appeared in both cells within 5 days. Many DNA fragments that were homologous to those of SFTSV were detected in the culture supernatant of the cells inoculated in next-generation sequencing.

DNA amplified by conventional RT-PCR using either of 2 primer pairs showed the expected sizes of 458 or 461 bp in agarose-electrophoresis (data not shown). The inoculated Vero cells were tested for the presence of SFTSV antigen in indirect IFA with rabbit anti-SFTSV rNP serum and showed a similar positive reactivity (Figure 1A). Enveloped and spherical virions with approximate diameters of 100 nm were detected by electron microscopy (Figure 1B). The morphology of the virion is compatible with that of a bunyavirus. The virus isolated from the patient was named SFTSV YG1.

Autopsy findings included right axillary lymphadenopathy ( $3.5 \times 2.0\ \text{cm}$ ; Figure 2A), bilateral renal swelling, mild retention of pericardial fluid (140 mL), and hepatic steatosis. Gastric ulceration was also observed in the pyloric region.

Severe necrotizing lymphadenitis with massive necrosis, the depletion of small lymphocytes, and severe infiltration of the swollen right axillary and right cervical lymph nodes by histiocytes and immunoblasts were observed (Figure 2B and 2C). Necrosis, which comprised nuclear debris and eosinophilic ghosts but not granulocytes, was distributed throughout the cortical area, the sinuses, and the capsule of the lymph node and had spread to the perinodal adipose tissue. No clusters of epithelioid histiocytes, stellate microabscesses, or granulomas were observed. There were no obvious intranuclear or intracytoplasmic viral inclusions. Prominent hemophagocytosis was observed in these lymph nodes, the bone marrow, and the spleen (Figure 2D and 2E). The bone marrow was relatively hypocellular, with no reduction in the number of megakaryocytes. The liver showed mild microvesicular fatty changes in zone 3 and mild inflammation, comprising lymphocytes and macrophages, around the portal tracts. The kidney showed subepithelial hemorrhage within the renal pelvis (Figure 2F). Significant hemophagocytosis were also observed in the mediastinal, hilar, and abdominal lymph nodes with no evidence of necrosis (Figure 3A, 3C, and 3E). The findings in the remaining visceral organs were unremarkable.

Positive signals for SFTSV NP antigen were detected in the cytoplasm of blastic cells and necrotic regions in the cortical area of the right axillary lymph node (Figure 3B). Viral antigen-positive cells were also detected in the right cervical lymph nodes (Figure 3D) but not in the mediastinal lymph nodes (Figure 3F), regardless of the level of immunoblast infiltration and hemophagocytosis (Figure 3E). Relatively few SFTSV antigen-positive cells were detected in the bone marrow, adrenal glands, the liver, and the spleen (Figure 3G–J), with no notable cytopathic effects or necrosis. No antigen-positive cells were detected in the heart, lungs, kidneys, gastrointestinal tract, aorta, or iliopsoas muscle.

The SFTSV genome, SFTSV genomic RNA (negative-strand RNA; Figure 4A), and mRNA (positive-strand RNA; Figure 4B) were detected in the blastic cells in the right cervical lymph node by ISH-AT analysis [18–20], while no signals were detected using an irrelevant probe as a negative control (Figure 4C). No signals showing necrotizing lymphadenitis without SFTSV infection were detected in the lymph nodes (negative control; Figure 4D).

SFTSV RNA was present, with high copy numbers, in the right axillary and cervical lymph node sections (Supplementary Table 3). Consistent with immunohistochemical analysis results, low copy numbers (100–1000 copies) of SFTSV RNA were also detected in the bone marrow, the spleen, the liver, and the adrenal glands. A few copies ( $<100$ ) were detected in other tissue sections that did not contain antigen-positive cells (as assessed by immunohistochemical analysis), suggesting that quantitative real-time RT-PCR detected cell-free circulating SFTSV; a high viral load in the serum is characteristic of SFTS infection [22]. The number of SFTSV RNA copies/cell was calculated using the  $\beta$ -actin mRNA copy number, estimated at 1500 copies/cell [17]. The SFTSV RNA copy numbers in the right axillary and cervical lymph node sections were the highest among the tissues tested, while the bone marrow, spleen, and liver showed relatively lower copy numbers per cell (Supplementary Table 3).

#### The Retrospective Study

Serum samples collected from 23 patients who were retrospectively suspected of having SFTS were sent to the Department of Virology 1, NIID (Figure 5). The male-to-female ratio was 18:5. The earliest infection dated back to 2005 (Figure 5B). Serum samples collected from 21 patients (for 2 patients, acute phase serum samples were not available for virologic analysis) were subjected to virus isolation and RT-PCR for amplification of the SFTSV genome. Serum samples collected from all 23 patients were tested for IgG and immunoglobulin M (IgM) antibodies to SFTSV in the indirect IFA. Of the 23 patients, 8 men and 2 women received a diagnosis of SFTS: 7 had positive results of virus isolation and genome amplification tests; 1 had positive results of virus genome amplification testing and IgM

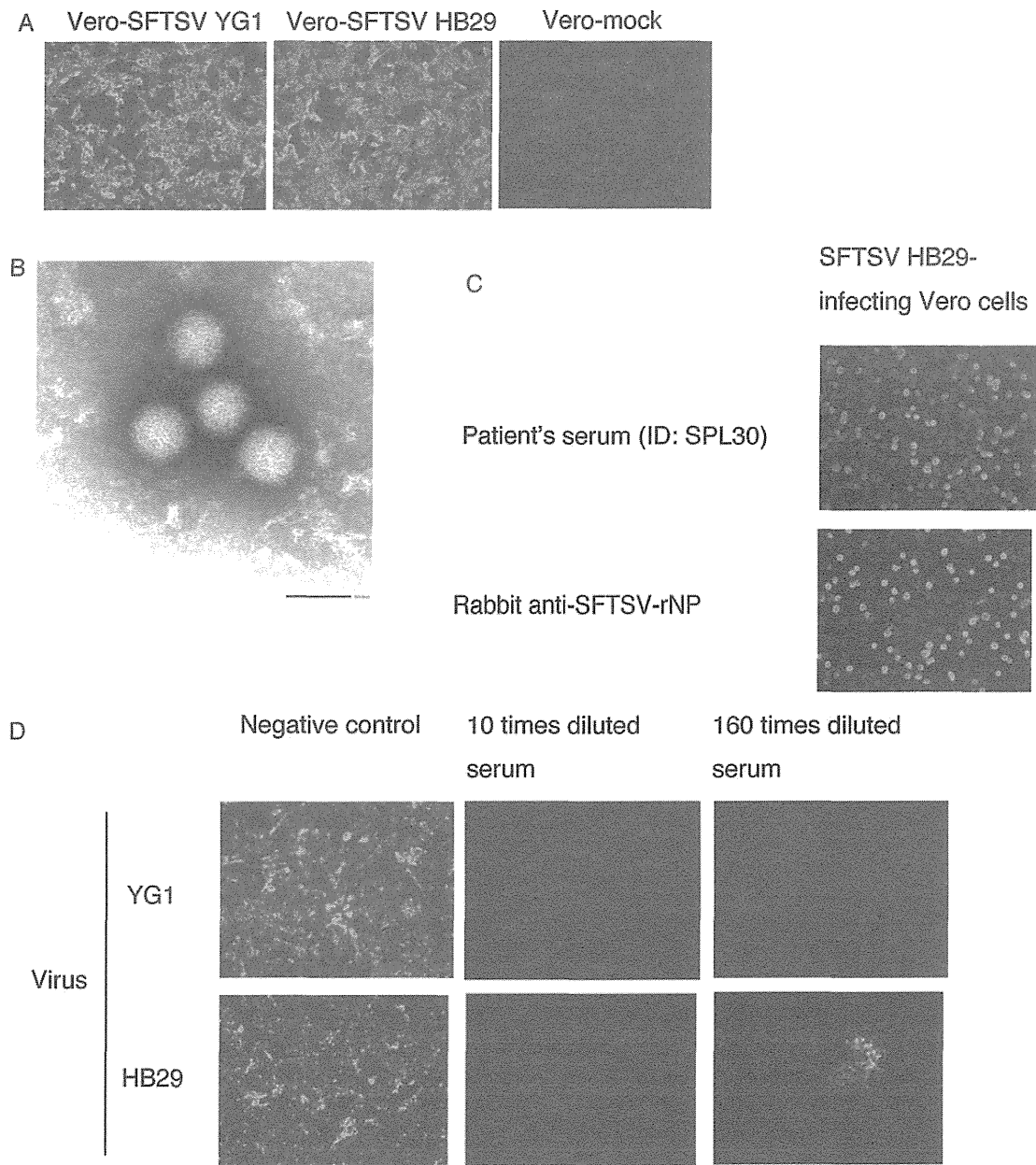


**Figure 1.** Reactivity of patient sera samples to severe fever with thrombocytopenia syndrome virus (SFTSV). *A*, Detection of SFTSV antigen in Vero cells by indirect immunofluorescence assay (IFA) with rabbit anti-SFTSV recombinant nucleoprotein (rNP) serum. *B*, Virions in the culture supernatant detected by electron microscopy (bar in the image indicates the length of 100 nm, ID: SPL004). *C*, Positive indirect IFA results of the serum collected from a surviving patient (ID: SPL030) in the convalescent phase of SFTSV HB29. *D*, Neutralizing antibody activity was induced in the serum collected from a patient (ID: SPL032) in the convalescent phase of SFTSV YG1 and SFTSV HB29.

antibody to SFTSV but had negative results of virus isolation analysis; and 2 were positive for IgG antibody to SFTSV. In the present study, the 2 patients who tested positive for SFTSV on the basis of detection of IgG to SFVSV were regarded as SFTS positive because their symptoms were reminiscent of SFTS and because reports of asymptomatic cases in China are quite rare

[23, 24]. For the purposes of the present study, the first patient was included with the 10 retrospective cases, for a total of 11 diagnosed cases.

All of the 11 patients in whom SFTS was diagnosed were aged  $\geq 50$  years (Figure 5A) and came from western Japan (Figure 5D). Disease onset occurred in all patients between the

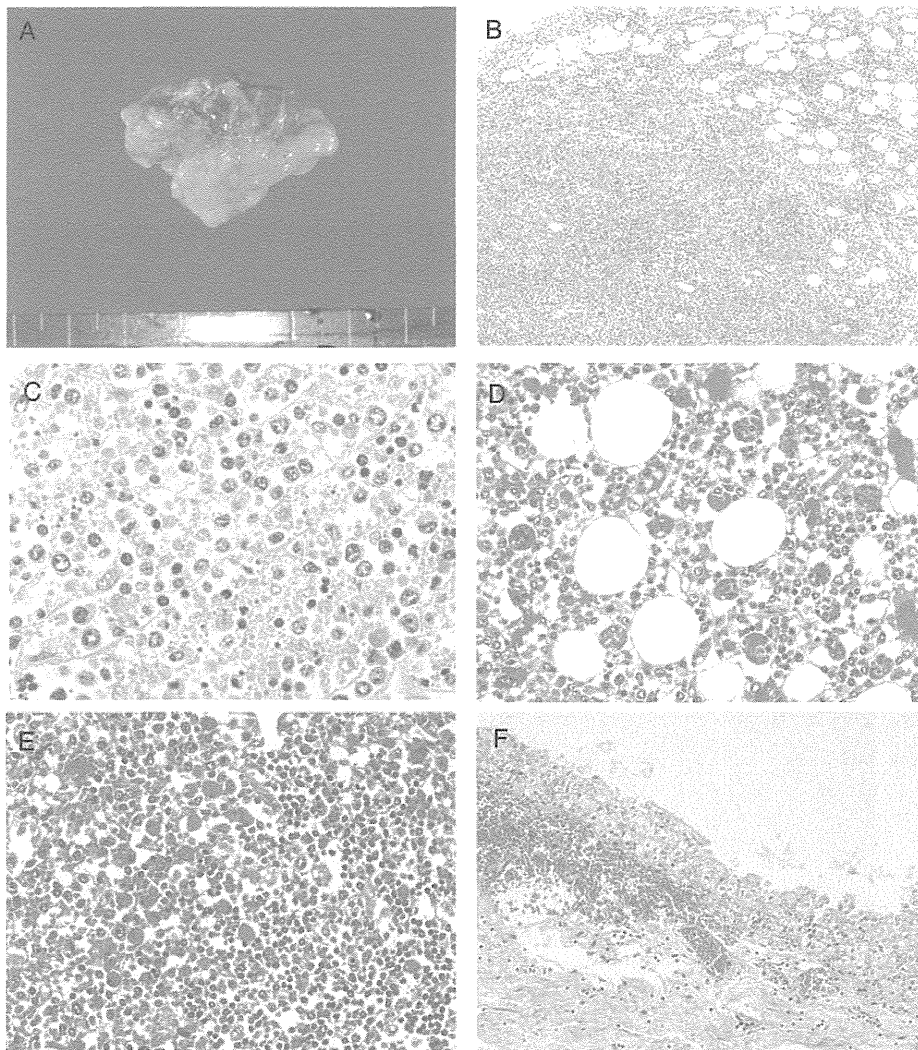


**Figure 2.** Macroscopic and microscopic findings under hematoxylin-eosin staining. *A*, Gross appearance of the swollen right axillary lymph node (3.5 × 2.0 cm). *B* and *C*, Microscopic findings in the right axillary lymph node. The basic architecture of the lymph node has been replaced by massive necrosis. The necrotic regions contain histiocytes, immunoblasts, nuclear debris, and eosinophilic ghosts but no neutrophils. *D* and *E*, Marked erythrophagocytosis in the bone marrow (*D*) and spleen (*E*). *F*, Acute subepithelial hemorrhage in the renal pelvis.

months of April and December (Figure 5C). Six of the 11 cases were fatal. There was clear evidence of tick bite in 2 cases.

#### Clinical Manifestation of 11 SFTS Patients

The clinical manifestations observed in SFTS patients are summarized in Table 1. All patients showed nonspecific febrile symptoms with gastrointestinal tract symptoms in the early phase of the disease. Deterioration in consciousness, characterized by dysarthria, disorientation, and alteration in consciousness, was commonly observed. Generalized convulsions were seen in the late stages of the disease in 5 of the 6 fatal cases. Respiratory symptoms were rarely observed. Superficial lymphadenopathy was detected in 5 patients.

Hemorrhagic symptoms such as petechiae, purpura, melena, bloody vomit, gingival bleeding as a form of discharge, and excessive bleeding at the site of skin biopsy were observed in 9 of the 11 patients.

Blood urea nitrogen and creatinine levels were elevated in 8 of 11 patients. Hematuria and proteinuria were observed in most patients.

In all 5 patients for whom bone marrow observation was performed, hemophagocytosis, with or without bone marrow cell dysplasia, was observed. The ferritin level was elevated in the blood of 8 patients, including the 5 in whom bone marrow examination was performed. Abnormalities were observed in tests in all of the patients for coagulopathy, prothrombin time,

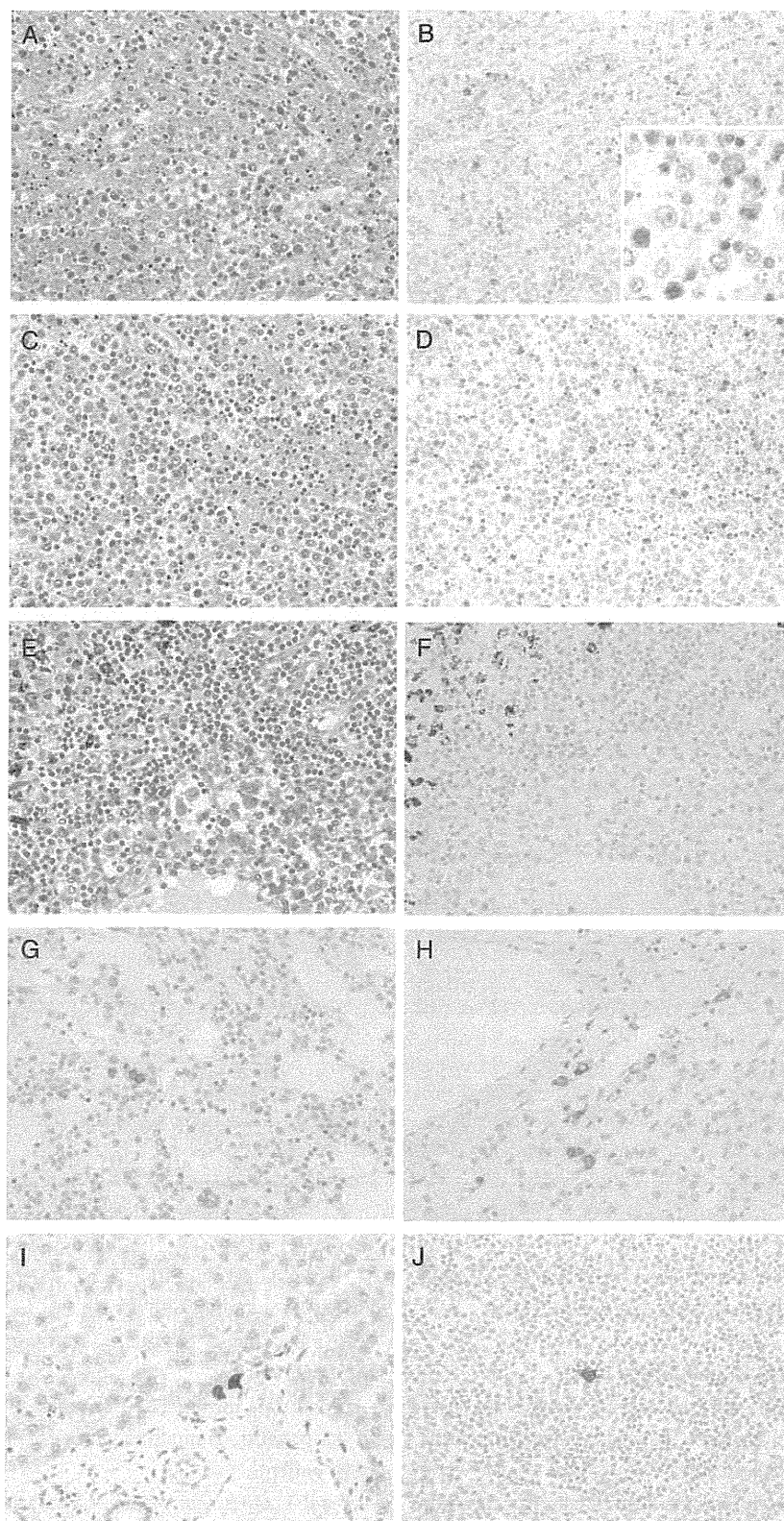


**Figure 3.** Microscopic and immunohistochemical tissue images. Hematoxylin-eosin staining (*A*, *C*, and *E*) and subsequent immunohistochemical analysis reveal the presence of severe fever with thrombocytopenia syndrome virus (SFTSV) NP (*B*, *D*, *F*, *G*, *H*, *I*, and *J*) in the right axillary (*A* and *B*), right cervical (*C* and *D*), and the mediastinal (*E* and *F*) lymph nodes. *A*, *C*, and *E*, Infiltration by immunoblasts and prominent hemophagocytosis was generally observed in the right axillary, right cervical, mediastinal, hilar, and abdominal lymph nodes; however, necrosis was only observed in the right axillary and cervical lymph nodes. *B*, *D*, and *F*, Viral antigen-positive cells were detected in the right axillary and cervical lymph nodes. Positive signals for SFTSV NP

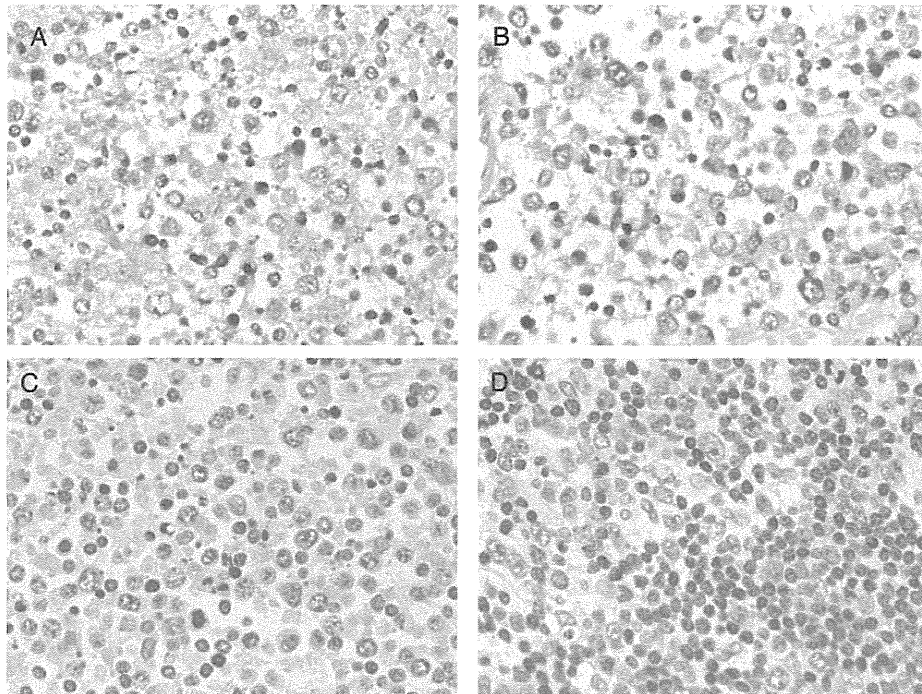


**Figure 4.** Detection of severe fever with thrombocytopenia syndrome virus (SFTSV) RNA in the right cervical lymph node by the in situ hybridization AT-tailing method. *A*, SFTSV genomic RNA was detected in the right cervical lymph node by the in situ hybridization AT-tailing method and a sense probe. SFTSV genomic RNA was detected in the cytoplasm of the blastic cells. *B*, The in situ hybridization AT-tailing method with an anti-sense probe detected a few cells in the right cervical lymph node that were positive for SFTSV messenger RNA (mRNA). SFTSV mRNA was also detected in the cytoplasm of blastic cells. *C*, No signals were detected in the right axillary lymph node by the in situ hybridization AT-tailing method with an irrelevant probe (negative control). *D*, A SFTSV sense probe detected no signals in lymph node sections showing necrotizing lymphadenitis without SFTSV infection.

activated partial thromboplastin time, fibrin/fibrinogen degradation products, fibrinogen, and/or D-dimer.

#### Phylogenetic Analysis

The Japanese SFTSV strains were closely related to the SFTSV Chinese isolates but formed an independent cluster for each segment (Figure 6). No geographic or chronological relationship was found between the Japanese and Chinese strains.

#### Neutralizing Antibody Response to SFTSV

Sera collected from the 5 surviving patients with SFTS in the convalescent phase showed neutralizing activities to SFTSV Japanese isolate YG1 (Figure 1*D*). The sera of these 5 patients also showed similar degrees of neutralizing activities to SFTSV HB29.

## DISCUSSION

The clinical manifestations of Japanese SFTS were very similar to those of severe cases of Chinese SFTS [1, 2], but the case-fatality rate (6 of 11 patients [55%]) was apparently higher than that in China, where an average of 12% of cases were fatal. It is worth noting that the characteristics of Japanese SFTS presented in this study were based on a limited number of patients and a strict case definition.

To our knowledge, this may be the first report describing the pathologic findings of a patient with SFTS. The local lymph nodes, which were the primary target organ in the first patient, served as the site of virus replication and showed marked pathologic changes, including massive necrosis. No neutrophil infiltration was observed in the patient. The spleen, liver, adrenal

*Figure 3 continued.* antigen were detected in the cytoplasm of blastic cells (B; inset). Inset shows a higher magnification (40×). In contrast, no signals were detected in the mediastinal lymph nodes, regardless of immunoblast infiltration and hemophagocytosis. G, H, I, and J, Immunohistochemical analysis of SFTSV NP was performed in the bone marrow (G), adrenal glands (H), liver (I), and spleen (J). A few SFTSV antigen-positive cells were observed in these tissues, with no notable cytopathic effects or necrosis (magnification, 20×; inset, 40×).



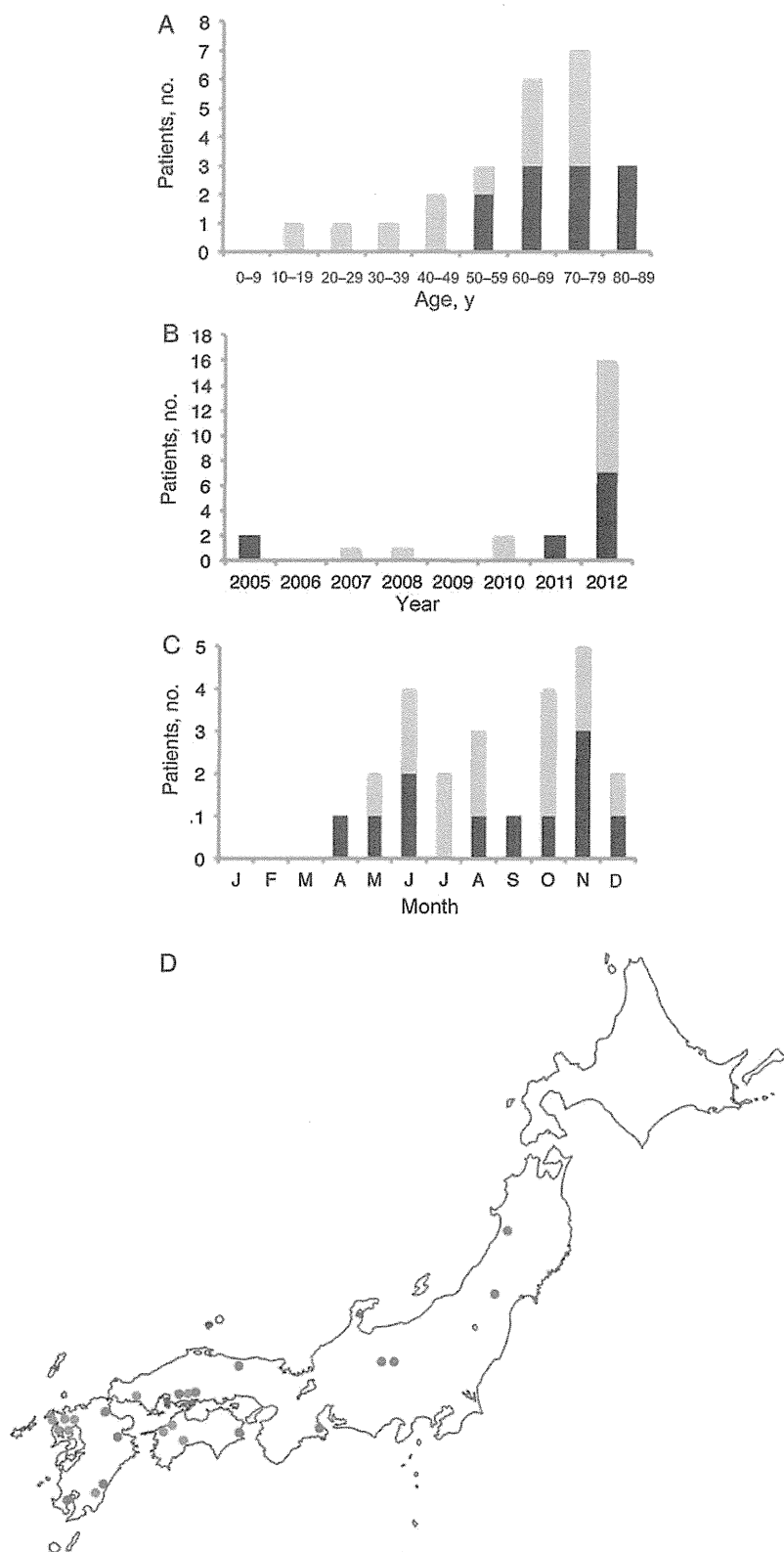


**Figure 5.** Chronological (*A*), age-based (*B*), geographic (*C*), and seasonal (*D*) distributions of patients with retrospectively diagnosed severe fever with thrombocytopenia syndrome (SFTS) in Japan. Black and gray bars in panels *A–C* indicate patients with and those without SFTS, respectively. The red and blue circles in panel *D* indicate the areas where patients with and those without SFTS were located.

**Table 1. Summary of Clinical Manifestation of Retrospectively Diagnosed Japanese Severe Fever With Thrombocytopenia Syndrome Cases**

Symptom or Laboratory Parameter	Variable (n = 11)
Clinical manifestation, positive/negative/unknown	
Fever	11/0/0
General symptoms	
General fatigue	11/0/0
Myalgia	2/5/4
Arthralgia	1/6/4
Headache	6/4/1
Gastrointestinal tract symptoms	
Overall	11/0/0
Nausea	9/2/0
Vomiting	6/5/0
Abdominal pain	6/5/0
Diarrhea	7/4/0
Anorexia	11/0/0
Respiratory symptoms	
Overall	3/8/0
Throat pain	2/9/0
Cough	1/10/0
Neurologic symptoms	
Overall	10/1/0
Dysarthria	3/8/0
Consciousness disturbance	8/3/0
Seizure	6/5/0
Hemorrhage	
Overall	9/2/0
Hemoptysis	1/10/0
Purpura	3/8/0
Bloody diarrhea	4/7/0
Gingival bleeding	5/6/0
Nasal hemorrhage	0/1/1/0
Genitourinary tract hemorrhage	0/1/1/0
Others	
Lymphadenopathy	5/6/0
Laboratory finding, no. (%)	
Total blood cell count	
Leukopenia	11 (100)
Thrombocytopenia	11 (100)
Serum chemistry	
Total protein level < 6.0 mg/dL (hypoproteinemia)	3 (27)
Albumin level < 3.0 mg/dL (hypoalbuminemia)	1 (9)
Aspartate aminotransferase level >30 IU/L	11 (100)
Alanine aminotransferase level >30 IU/L	11 (100)
Lactate dehydrogenase level >250 IU/L	11 (100)
Creatine kinase level >200 IU/L	11 (100)
Blood urea nitrogen level >20 mg/dL	7 (64)
Creatinine level >1 mg/dL	7 (64)
Inflammatory parameter	
C-reactive protein level >1 mg/dL	3 (27)

Table 1 continued.

Symptom or Laboratory Parameter	Variable (n = 11)
Urinalysis	
Hematuria	9 (90) <sup>a</sup>
Proteinuria	10 (100) <sup>a</sup>
Coagulopathy, no. (%)	
Abnormality in either DIC parameter <sup>b</sup>	11 (100)
Hemophagocytosis, no. (%)	
Bone marrow examination	
Hemophagocytosis	5 (100) <sup>c</sup>
Positive increased ferritin level	8 (100) <sup>d</sup>
Tick bite within 2 weeks of onset, no. (%)	2 (18)

<sup>a</sup> Basic number is 10.

<sup>b</sup> Disseminated intravascular coagulation (DIC) parameters include prothrombin time, activated partial thromboplastin time, and levels of antithrombin 3, fibrinogen, D-dimer, and fibrinogen degradation products.

<sup>c</sup> Basic number is 5.

<sup>d</sup> Basic number is 8.

glands, and bone marrow contained a few SFTSV-infected cells. However, no viral antigens were detected in hepatocytes or in the parenchymal cells of the adrenal glands. Viruses belonging to the *Bunyaviridae* family, which includes the Rift valley fever virus, Hantaan virus, and Heartland virus [10], infect monocytes/macrophages [25, 26]. These cells may control the spread (or containment) of viruses to cells within other organs. The pathologic and virologic observations suggest that SFTSV replicated in the blastic cells within the lymph nodes and that replication took place predominantly in the local lymph nodes, not in the major organs.

Macrophages with phagocytosis of bone marrow cells were observed in all of the patients in whom bone marrow examination was performed. Furthermore, pathologic examination of the lymph nodes, bone marrow, and the spleen of the initial patient revealed marked hemophagocytosis, regardless of the presence of SFTSV-infected cells (Figure 2D and 2E and Figure 3A, 3C, and 3E). Ferritin level was extremely elevated in the sera of all patients who were tested. Abnormality in coagulopathy-associated indices was also observed in all patients. SFTSV infections induced a cytokine storm, the level of which was associated with the severity of SFTS [27]. These results indicate that in addition to multiorgan dysfunction, hemophagocytosis and disseminated intravascular coagulation are major factors for poor prognosis.

The mode of the natural SFTSV lifecycle in Japan should be clarified to enable better identification of risk factors for SFTSV infection and to address strategies for reducing the risk of infections. Further study is necessary to clarify the circulation of SFTSV in nature in Japan, in terms of tick species, percentages of SFTSV positivity for each tick species, and the prevalence of

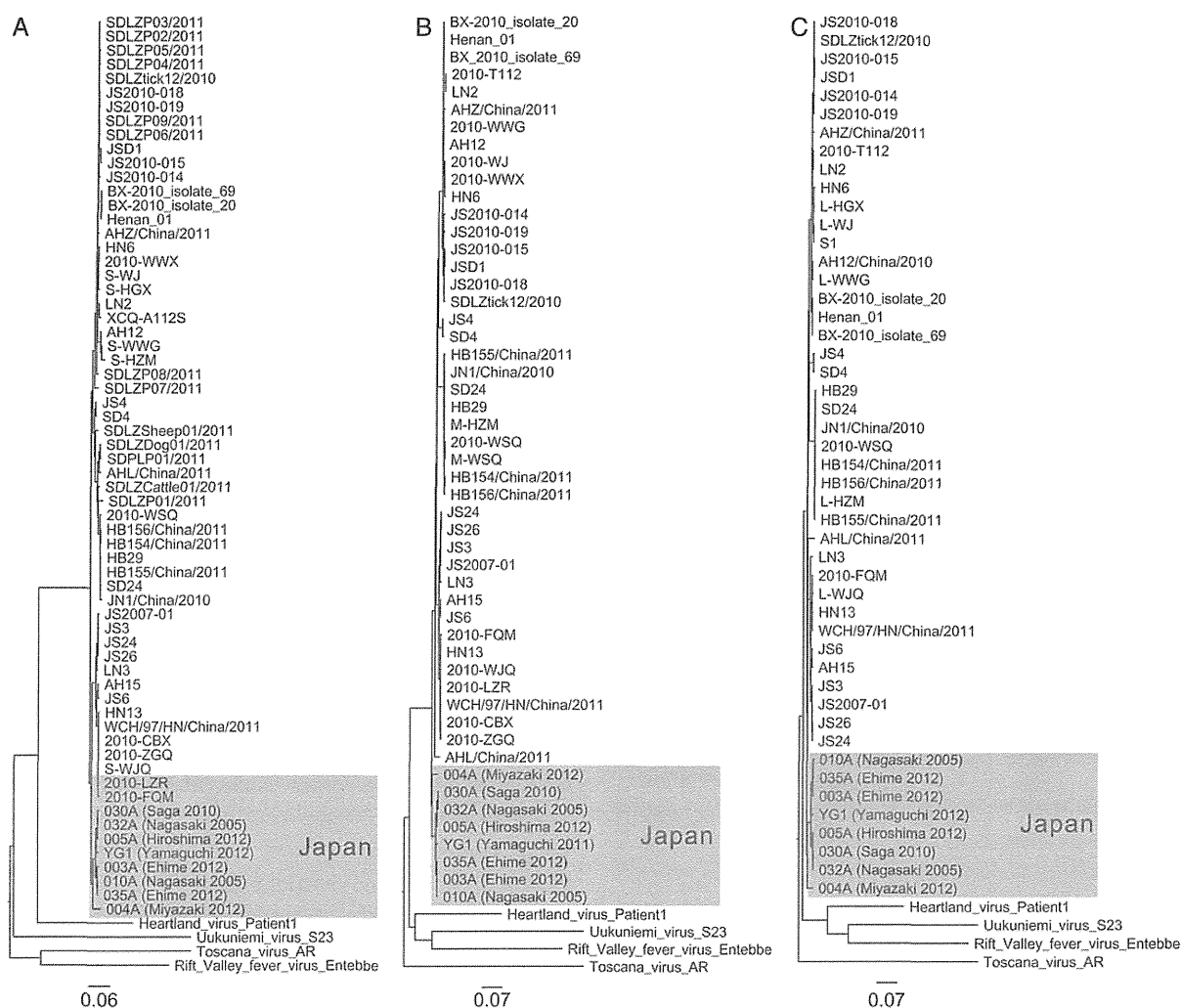


**Figure 6.** Phylogenetic trees showing the phylogenetic positions of severe fever with thrombocytopenia syndrome virus (SFTSV) strains in Japan, compared with other known strains. Trees are based on the S segment (A; left panel), M segment (B; middle panel), and L segment (C; right panel). Heartland virus, Uukuniemi virus, Toscana virus, and Rift Valley fever virus are included in the phylogenetic analyses.

SFTSV-positive ticks, to better determine and evaluate the risk factors for SFTSV infection in Japan.

Japanese isolates formed a cluster that was independent from Chinese isolates (Figure 6), indicating that SFTSV has been circulating in Japan naturally for some time. The earliest year for which we have evidence of SFTS in patient sera samples was 2005, and to our knowledge, the article by Liu et al, which concerns SFTS occurrence in China during 2006, reports the oldest cases from China [5]. It is also noteworthy that patients with SFTS were reported in South Korea in 2013 (ProMed mail: archive numbers 20130521.1729124 and 20130529.174441). The prevalence of SFTS in and around East Asia should be studied to clarify the nature of SFTS in the region.

In conclusion, SFTSV is prevalent in Japan. Japanese SFTSV strains have characteristics similar to those of Chinese isolates

but an independent genotype, which indicates that SFTSV has been present in Japan for some time.

### Supplementary Data

Supplementary materials are available at *The Journal of Infectious Diseases* online (<http://jid.oxfordjournals.org/>). Supplementary materials consist of data provided by the author that are published to benefit the reader. The posted materials are not copyedited. The contents of all supplementary data are the sole responsibility of the authors. Questions or messages regarding errors should be addressed to the author.

### Notes

**Acknowledgments.** We thank Dr De-Xin Li and Dr Mi-Fang Liang, National Institute for Viral Disease Control and Prevention, Chinese Center for Disease Control and Prevention, Beijing, PRC, for providing us with the SFTSV HB29 strain; Dr Roger Hewson, Virology, Pathogenesis, and



Emerging Disease, Public Health England–Microbiology Services, Porton Down, Salisbury, United Kingdom, for his critical comments; and the municipal officials who supported this work, in the prefectures in which patients with SFTS were reported.

**Financial support.** This work was supported by the Ministry of Health, Labor and Welfare Science Research (grants in aid H24-Shinko-Ippan-013, H22-Shinko-Ippan-006, and H25-Shinko-Shitei-009).

**Potential conflicts of interest.** All authors: No reported conflicts.

All authors have submitted the ICMJE Form for Disclosure of Potential Conflicts of Interest. Conflicts that the editors consider relevant to the content of the manuscript have been disclosed.

## References

- Xu B, Liu L, Huang X, et al. Metagenomic analysis of fever, thrombocytopenia and leukopenia syndrome (FTLS) in Henan Province, China: discovery of a new bunyavirus. *PLoS Pathog* **2011**; 7:e1002369.
- Yu XJ, Liang MF, Zhang SY, et al. Fever with thrombocytopenia associated with a novel bunyavirus in China. *N Engl J Med* **2011**; 364:1523–32.
- Zhang YZ, Zhou DJ, Qin XC, et al. The ecology, genetic diversity, and phylogeny of Huaiyangshan virus in China. *J Virol* **2012**; 86:2864–8.
- Jiang XL, Wang XJ, Li JD, et al. Isolation, identification and characterization of SFTS bunyavirus from ticks collected on the surface of domestic animals [in Chinese]. *Chin J Virol* **2012**; 28:252–7.
- Liu Y, Li Q, Hu W, et al. Person-to-person transmission of severe fever with thrombocytopenia syndrome virus. *Vector Borne Zoonotic Dis* **2012**; 12:156–60.
- Gai Z, Liang M, Zhang Y, et al. Person-to-person transmission of severe fever with thrombocytopenia syndrome bunyavirus through blood contact. *Clin Infect Dis* **2012**; 54:249–52.
- Bao CJ, Guo XL, Qi X, et al. A family cluster of infections by a newly recognized bunyavirus in eastern China, 2007: further evidence of person-to-person transmission. *Clin Infect Dis* **2011**; 53:1208–14.
- Chen H, Hu K, Zou J, Xiao J. A cluster of cases of human-to-human transmission caused by severe fever with thrombocytopenia syndrome bunyavirus. *Int J Infect Dis* **2013**; 17:e206–8.
- Tang X, Wu W, Wang H, et al. Human-to-human transmission of severe fever with thrombocytopenia syndrome bunyavirus through contact with infectious blood. *The J Infect Dis* **2013**; 207:736–9.
- McMullan LK, Folk SM, Kelly AJ, et al. A new phlebovirus associated with severe febrile illness in Missouri. *New Engl J Med* **2012**; 367:834–41.
- Saijo M, Niikura M, Morikawa S, et al. Enzyme-linked immunosorbent assays for detection of antibodies to Ebola and Marburg viruses using recombinant nucleoproteins. *J Clin Microbiol* **2001**; 39:1–7.
- Kitts PA, Possee RD. A method for producing recombinant baculovirus expression vectors at high frequency. *BioTechniques* **1993**; 14:810–7.
- Saijo M, Qing T, Niikura M, et al. Recombinant nucleoprotein-based enzyme-linked immunosorbent assay for detection of immunoglobulin G antibodies to Crimean-Congo hemorrhagic fever virus. *J Clin Microbiol* **2002**; 40:1587–91.
- Saijo M, Qing T, Niikura M, et al. Immunofluorescence technique using HeLa cells expressing recombinant nucleoprotein for detection of immunoglobulin G antibodies to Crimean-Congo hemorrhagic fever virus. *J Clin Microbiol* **2002**; 40:372–5.
- Saijo M, Ogino T, Taguchi F, et al. Recombinant nucleocapsid protein-based IgG enzyme-linked immunosorbent assay for the serological diagnosis of SARS. *J Virol Methods* **2005**; 125:181–6.
- Jin C, Liang M, Ning J, et al. Pathogenesis of emerging severe fever with thrombocytopenia syndrome virus in C57/BL6 mouse model. *Proc Natl Acad Sci USA* **2012**; 109:10053–8.
- Nakajima N, Hata S, Sato Y, et al. The first autopsy case of pandemic influenza (A/H1N1pdm) virus infection in Japan: detection of a high copy number of the virus in type II alveolar epithelial cells by pathological and virological examination. *Jpn J Infect Dis* **2010**; 63:67–71.
- Nakajima N, Ionescu P, Sato Y, et al. In situ hybridization AT-tailing with catalyzed signal amplification for sensitive and specific in situ detection of human immunodeficiency virus-1 mRNA in formalin-fixed and paraffin-embedded tissues. *Am J Pathol* **2003**; 162:381–9.
- Nakajima N, Asahi-Ozaki Y, Nagata N, et al. SARS coronavirus-infected cells in lung detected by new in situ hybridization technique. *Jpn J Infect Dis* **2003**; 56:139–41.
- Nakajima N, Sata T, Hanaki K, Kurata T, Yoshikura H. Application of the hybridization AT-tailing method for detection of human immunodeficiency virus RNA in cells and simian immunodeficiency virus RNA in formalin-fixed and paraffin-embedded tissues. *J Virol Methods* **1999**; 81:169–77.
- Kuramochi H, Hayashi K, Uchida K, et al. Vascular endothelial growth factor messenger RNA expression level is preserved in liver metastases compared with corresponding primary colorectal cancer. *Clin Cancer Res* **2006**; 12:29–33.
- Huang X, Liu L, Du Y, et al. Detection of a novel bunyavirus associated with fever, thrombocytopenia and leukopenia syndrome in Henan Province, China, using real-time reverse transcription PCR. *J Med Microbiol* **2013**; 62:1060–4.
- Zhao L, Zhai S, Wen H, et al. Severe fever with thrombocytopenia syndrome virus, Shandong Province, China. *Emerg Infect Dis* **2012**; 18:963–5.
- Cui F, Cao HX, Wang L, et al. Clinical and epidemiological study on severe fever with thrombocytopenia syndrome in yiyuan county, Shandong province, China. *Am J Trop Med Hyg* **2013**; 88:510–2.
- Lewis RM, Morrill JC, Jahrling PB, Cosgriff TM. Replication of hemorrhagic fever viruses in monocytic cells. *Rev Infect Dis* **1989**; 11(Suppl 4):S736–42.
- Nagai T, Tanishita O, Takahashi Y, et al. Isolation of haemorrhagic fever with renal syndrome virus from leukocytes of rats and virus replication in cultures of rat and human macrophages. *J Gen Virol* **1985**; 66(Pt 6):1271–8.
- Sun Y, Jin C, Zhan F, et al. Host cytokine storm is associated with disease severity of severe fever with thrombocytopenia syndrome. *J Infect Dis* **2012**; 206:1085–94.



